

# Simultaneous $T_1$ , $T_2$ , and $B_1$ Mapping Using Partially RF-Spoiled Gradient Echo

Y. Taniguchi<sup>1</sup>, S. Yokosawa<sup>1</sup>, and Y. Bito<sup>1</sup>

<sup>1</sup>Central Research Laboratory, Hitachi, Ltd., Kokubunji, Tokyo, Japan

## Introduction

Quantitative parametric mapping in MRI is used to obtain distributions of MR parameters such as  $T_1$  and  $T_2$  relaxation times. MR parameters are estimated from MR images obtained with various acquisition parameters of a pulse sequence. For example, a  $T_1$  map is estimated from images acquired by an inversion recovery sequence with various  $TIs$  (inversion times), and a  $T_2$  or  $T_2^*$  map is estimated from images acquired with various  $TEs$  (echo times) by multiple spin-echo or gradient-echo (GrE) sequences. In the  $T_1$  estimation at a magnetic field strength of 3T or higher, the effect of  $B_1$  distribution also needs to be estimated.

In the estimation, the intensity function, which defines the relationship of image intensity to acquisition and MR parameters, is used to find MR parameter values that lead to a best fit of the intensity function to image intensity values as a function of acquisition parameters. The intensity function thus needs to be formulated analytically in a simple form. Therefore, the applicable pulse sequence is limited, and this makes it difficult to acquire images rapidly and to obtain multiple MR parameters simultaneously. We have proposed a method to formulate the intensity function numerically by using a computer simulation based on the Bloch equations [1]. The intensity function of rapid imaging of RF-spoiled GrE was formulated using this method and was successfully applied for  $T_1$  and  $B_1$  mapping.

It is also possible to simultaneously obtain multiple MR parameter maps such as  $T_1$  and  $T_2$  maps by applying a pulse sequence in which the intensity depends on these MR parameters. In this paper, we formulate the intensity function for simultaneous estimation of  $T_1$ ,  $T_2$ , and  $B_1$  maps by using partially RF-spoiled GrE in which the intensity depends on  $T_2$  in addition to  $T_1$  by changing the RF phase in RF-spoiled GrE. We confirmed that these three maps were well estimated from images obtained in a phantom experiment.

## Method

A schematic diagram of the pulse-sequence simulator used to formulate the intensity function is shown in Fig. 1. The inputs to the simulator are the subject model (as distributions of density of spins with relaxation times  $T_1$  and  $T_2$ ) and the pulse sequence. The Bloch equations are solved for each spin in the subject model at an arbitrary time, according to the given pulse sequence. In solving the equations, the transition-matrix method and an analytical solution are used, and the effects of  $T_1$  and  $T_2$  are factored into both calculations [2]. The echoes are then obtained by calculating the vector sum of the spins.

This simulator was used to formulate the intensity function for partially RF-spoiled GrE. This sequence is a fast and efficient pulse-sequence, and its intensity function is formulated analytically; however, the function is not simple enough for estimation of MR parameters. The subject model is shown in Fig. 2, where the spin density was uniform while  $T_1$  and  $T_2$  were distributed from 50 – 3000 ms in the x direction and 30 – 1500 ms in the y direction, respectively. The image contrast of partially RF-spoiled GrE depends on the acquisition parameters of repetition time ( $TR$ ), flip angle ( $FA$ ), and phase cycling of RF ( $\theta$ ). Three-hundred images with different contrast were acquired by the simulator with different  $TR$ ,  $FA$ , and  $\theta$  values: 10, 15, 20, 25, and 30 ms for  $TR$ , 1, 3, 4, 10, 15, 20, 30, 40, 50, and 60 degrees for  $FA$ , and 0, 1, 3, 5, 8, and 12 degrees for  $\theta$ . The intensity function  $f(T_1, T_2, TR, FA, \theta)$  was formulated numerically by cubic polynomial interpolation of the intensity of these images.

MR parameter values of  $T_1$ ,  $T_2$ , and  $B_1$  were estimated using the intensity function in a phantom experiment on a 1.5T MRI system. The phantom, as shown in Fig. 3, was composed of solutions of NiCl in water with four different concentrations: 1, 1.5, 2.5, and 5 mM with respective relaxation times ( $T_1$ ,  $T_2$ ) of (1036, 813), (745, 596), (466, 384), and (297, 254) ms. Sixteen optimal parameter sets were selected from twenty combinations of  $FA$  and  $\theta$ : 10, 20, 30, 40, and 50 degrees for  $FA$  and 0, 2, 6, and 12 degrees for  $\theta$  using the law of error propagation with target parameters  $T_1$  and  $T_2$  of 800 ms (Fig. 4).  $TR$  was fixed at 20 ms. Other acquisition parameters were as follows—matrix size: 128×128, field of view: 250 mm,  $TE$ : 5 ms, and bandwidth: 20 kHz. Least squares fits were then found with the following equation to obtain values of  $T_1$ ,  $T_2$ ,  $B_1$ , and  $a$ :

$$\chi^2 = \sum_{\theta} \sum_{TR} \sum_{FA} \left\{ \frac{I(TR, FA, \theta) - a f(T_1, T_2, B_1, FA, TR, \theta)}{I(TR, FA, \theta)} \right\}^2 = \min,$$

$$0.05 < T_1 < 3, 0.03 < T_2 < 1.5, 0.5 < B_1 < 1.2, 0 < a,$$

where  $I(TR, FA, \theta)$  is the intensity of the phantom images, and  $a$  is a coefficient representing spin density and receiver coil sensitivity.

## Results and Discussion

The results of  $T_1$  and  $T_2$  mapping obtained by the estimation are shown in Fig. 5 and Table 1, and the estimated  $B_1$  and  $a$  are shown in Fig. 6. In Fig. 6, a  $B_1$  map obtained by using the double-angle method (DAM), and coil sensitivity are also shown for comparison. In Fig. 5 and Table 1, it is confirmed that  $T_1$  and  $T_2$  values are well estimated and that the errors of the values are less than or equal to 9% and 14%, respectively. The  $B_1$  map is also well estimated compared with DAM, as shown in Fig. 6.

The parameter of  $a$  is possibly proportional to the coil sensitivity because the subject is a phantom with an almost uniform density. In a comparison between  $a$  and coil sensitivity in Fig. 6, it is clear that  $a$  is slightly smaller than coil sensitivity at the periphery of the field of view, but they agree in the tendency for the amplitude to decrease toward the center of the field of view.

We also estimated  $T_1$ ,  $T_2$ , and  $B_1$  values with a  $TR$  of 10 ms instead of 20 ms. In this case, the value of the objective function of the error propagation was worse, and only the long  $T_2$  value (813 ms) was not correctly estimated (estimated  $T_2$  was 611 ms). The other values were well estimated, as was the case with a  $TR$  of 20 ms. The reason for this is that the  $T_2$  decay is small in the case of a short  $TR$  (10 ms), and the intensity function does not depend on  $T_2$  enough to estimate a long  $T_2$ . It is necessary to evaluate the estimation using the sequence parameter of a longer  $TE$  than 5 ms to enable  $TR$  to decrease for faster acquisition.

## Conclusion

We have confirmed that our proposed method can be applied to estimate  $T_1$ ,  $T_2$ , and  $B_1$  maps simultaneously using a fast pulse sequence of partially RF-spoiled GrE. The estimation is based on the intensity function formulated numerically by computer simulation.

## References

- [1] Taniguchi, Y et al., ISMRM, 3113, 2010.
- [2] Taniguchi, Y et al., Systems and Computers in Japan, 26: 54, 1995.

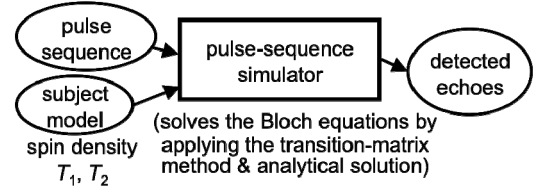


Fig. 1: Pulse-sequence simulator.

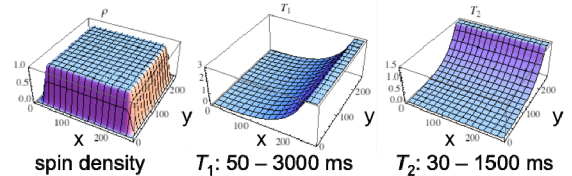


Fig. 2: Subject model for pulse-sequence simulation.

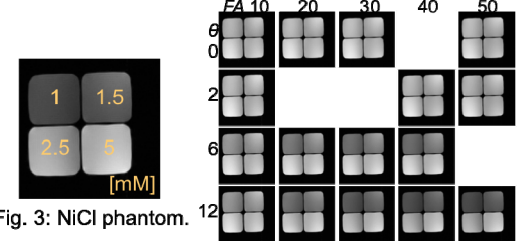


Fig. 3: NiCl phantom.

Fig. 4: images selected for estimation.

NiCl [mM]	$T_1$ [ms]	$T_2$ [ms]
1	1129±29 (+8.9%)	758±35 (-6.7%)
1.5	808±22 (+8.4%)	557±23 (-6.5%)
2.5	479±13 (+2.8%)	353±13 (-7.9%)
5	299±12 (+0.6%)	219±8 (-14%)

mean±SD (error%)

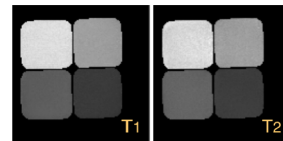


Fig. 5:  $T_1$  and  $T_2$  maps.

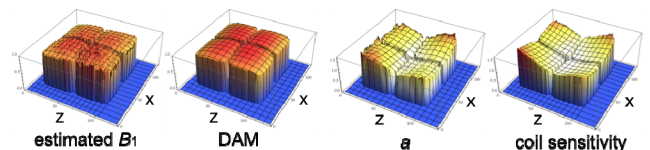


Fig. 6: Estimated  $B_1$  map and  $a$ , and their comparison with DAM and coil sensitivity.